Computational and experimental investigation of dynamic shock reflection phenomena

K Naidoo* **and B W Skews**

School of Mechanical Engineering, University of the Witwatersrand, Johannesburg, 2050, South Africa

Summary. This paper reports the development of an experimental facility for the investigation of dynamic, two-dimensional shock reflection phenomena generated by a rapidly pitching wedge in proximity of an ideal wall. CFD simulations of the rapidly pitching wedge are used to analyse dynamic flow field phenomena and response of the triple point below and within the dual solution domain. Computed, unsteady pressure traces on the reflection plane are also analysed.

1 Introduction

Consider the shock wave reflection pattern generated by a wedge of infinite span in close proximity to an ideal wall. The regular reflection (RR) and Mach reflection (MR) configurations possible in a steady supersonic freestream are well known, as well as the steady state transition criteria between these configurations. Transition criteria for the steady, two-dimensional case were published by Ben-Dor [1]. These transition criteria are not valid for the rapidly pitching wedge in which there are significant dynamic effects. Transition between RR and MR and other unsteady phenomena observed for the rapidly pitching, two-dimensional wedge was presented by Felthun and Skews [2] and Naidoo and Skews [3].

This research paper documents progress on the development of an experimental test rig for the investigation of unsteady shock reflection phenomena. Computational fluid dynamics (CFD) was used to investigate some of the unsteady flow field phenomena. An analysis of the computed unsteady flow field, triple point response and the static pressure traces on the reflection plane is presented.

2 Experimental facility development

A facility is being developed for the experimental investigation of two-dimensional, unsteady shock reflection phenomena generated by a rapidly pitching wedge in close proximity to an ideal wall (Fig. 1). This facilty is being developed for the 450mm x 450mm supersonic blow-down wind tunnel at the Council for Scientific and Industrial Research, South Africa. The rig consists of two wedges positioned symmetrically about a horizontal plane, to simulate the effect of an ideal, smooth reflection surface. A large wedge aspect ratio of 4.5 was used to ensure approximate two-dimensional flow on the wedge centre plane. The motion of both wedges is synchronized to maintain a horizontal symmetry plane.

* Present Address: CSIR - Defence Peace Safety and Security, Aeronautics Systems Competency, PO Box 395, Pretoria, 0001, South Africa

Currently, the rig is only capable of gradual wedge pitch rates to approximate the steady state case. This rig will be modified for rapid rotation of the wedges and will be achieved with a spring loaded actuator. The mechanism has been designed to achieve instantaneous maximum pitch rates of approximately 25000.0 deg/s. Tests were conducted to generate steady state, reference flow field data at freestream Mach numbers, $M_\infty = 2.0$ and $M_\infty = 3.0$. Flow visualization was achieved with three-colour schlieren (Fig. 2). Flow field images will be acquired with a high speed digital camera for the dynamic tests.

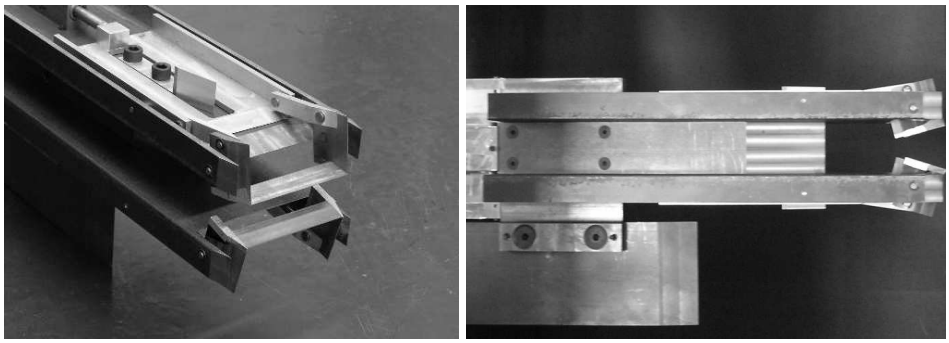

Fig. 1. Experimental test rig for the investigation of dynamic shock reflection phenomena

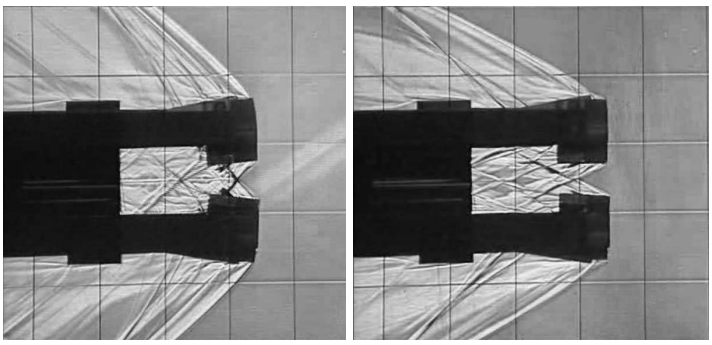

Fig. 2. Three-colour schlieren images captured during reference tests

3 Numerical simulations

Euler simulations in Table 1 were carried out with a vertex centred, Arbitrary Lagrangian Eulerian, finite volume scheme on unstructured triangular meshes [2]. The numerical method enables dynamic adaptive refinement, ideally suited to moving boundary problems in supersonic flows. Steady state, supersonic freestream conditions were established before the wedge, of constant chord $w = 60.0$ mm, was pitched at a rapid and constant rate. Solutions were tested for grid dependence and a fine grid was used for all flow field computations. Any flow solution dependence on the fine grid is small compared to the

dynamic effects observed in this study. These test cases briefly explore the effect of M_∞, pitch rate and pitch direction on Mach stem growth, for fixed trailing edge separation, g, as well as fixed leading edge separation, h. Results are valid for the specified initial wedge incidence angle, θ_i. Maximum pitch rate, per freestream condition, was specified by scaling the wedge trailing or leading edge tangential speed, V_T, with the freestream acoustic speed, a_∞, i.e. $V_{Tmax} = 0.1a_\infty$.

Table 1. Dynamic test matrix, $\gamma = 1.4$

Case	M_∞	Pitch Rate ($^\circ/s$)	$\frac{g}{w}$	$\frac{h}{w}$	θ_i	Case	M_∞	Pitch Rate ($^\circ/s$)	$\frac{g}{w}$	$\frac{h}{w}$	θ_i
1	4.0	+8500.0	0.48	-	19.0	7	2.0	+12500.0	0.65	-	8.0
2	4.0	+17000.0	0.48	-	19.0	8	2.0	+25000.0	0.65	-	8.0
3	4.0	+17000.0	-	0.85	19.0	9	2.0	+25000.0	-	0.85	8.0
4	4.0	-8500.0	0.48	-	26.5	10	2.0	-12500.0	0.65	-	15.5
5	4.0	-17000.0	0.48	-	26.5	11	2.0	-25000.0	0.65	-	15.5
6	4.0	-17000.0	-	0.85	26.5	12	2.0	-25000.0	-	0.85	15.5

3.1 Flow field characterization

The computed flow field for case 12 is discussed here. Density contours for case 12 are shown in Fig. 3. A history of static pressure traces through the reflection point on the ideal wall are shown in Fig. 5. Mach stem height history is shown in Fig. 6(a).

A steady MR is established at wedge incidence, $\theta = 15.5^\circ$. The wedge is pitched instantaneously at -25000.0 deg/s about its leading edge. Initially, the triple point maintains its vertical position. The wedge surface is moving away from the reflection plane and a weak expansion region is setup on the wedge surface. At $\theta = 13.5^\circ$, the acoustic pulses from the moving wedge surface reach the triple point and the Mach stem height, m, increases. The Mach stem height reaches a maximum at approximately $\theta = 8.7^\circ$ and decreases subsequently. In case 12, the pitch rate and initial wedge incidence are such that the Mach stem height has a finite value at $\theta = 0.0^\circ$. The rapid pitch generates an inverse MR. This can be observed from Fig. 3(e) and Fig. 3(f), i.e. the shear layer is directed away from the wall. Also, the pressure traces in Fig. 5 show that while the reflection pattern is MR, the static pressure rise through the reflection point decreases with decreasing wedge incidence. At $\theta = 0.0^\circ$ the wedge sheds the shock wave system, hereafter referred to as the "orphan"shock system. The "orphan"shock system washes downstream below $\theta = 0.0^\circ$.

3.2 Transition of the "orphan"shock system

Just below $\theta = 0.0^\circ$, the "orphan"shock system maintains the basic anatomy of the oblique shock system previously attached to the wedge leading edge (Fig. 4). There still remains an incident oblique shock wave, a small Mach stem and a reflected oblique shock wave at $\theta = -0.5^\circ$. As the "orphan"shock system washes downstream the incident oblique

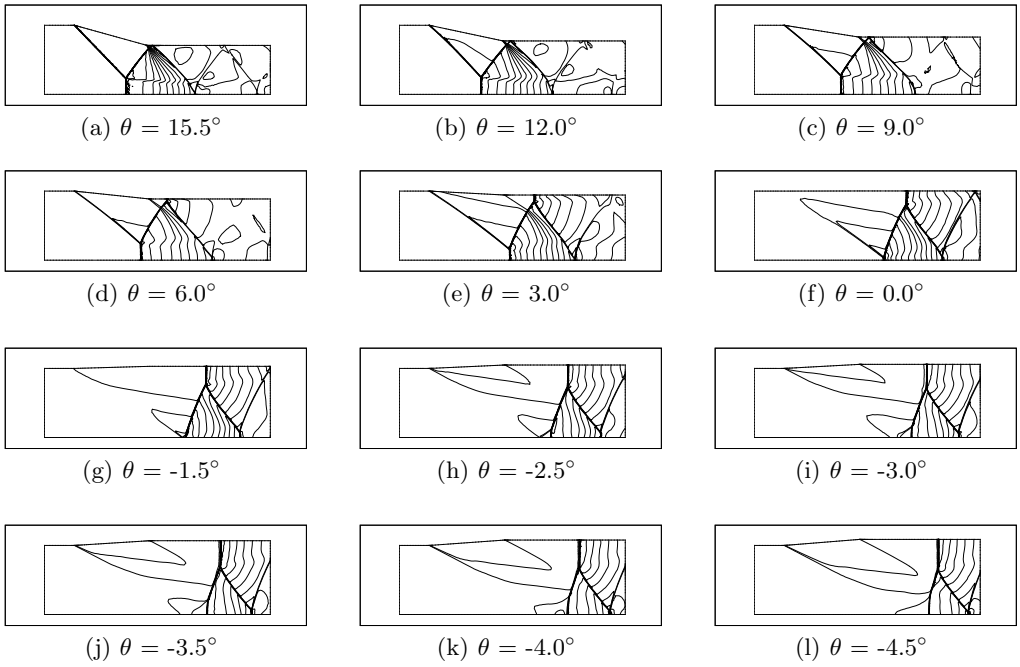

(a) θ = 15.5° (b) θ = 12.0° (c) θ = 9.0°

(d) θ = 6.0° (e) θ = 3.0° (f) θ = 0.0°

(g) θ = -1.5° (h) θ = -2.5° (i) θ = -3.0°

(j) θ = -3.5° (k) θ = -4.0° (l) θ = -4.5°

Fig. 3. Dynamic MR → RR : case 12

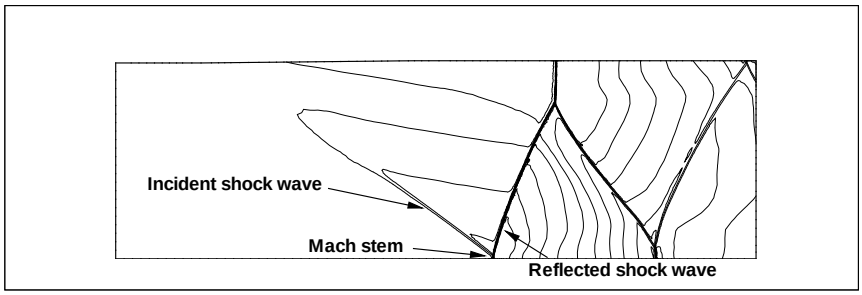

Fig. 4. Anatomy of the "orphan shock"system at θ = -0.5° : case 12

shock begins to diminish in strength (Fig. 5). At the same time the triple point continues to move toward the wall. At the time θ = -1.5° the "orphan"shock system transitions from MR to RR. There is a discontinuity in static pressure rise through the reflection point on the wall on transition from MR to RR due to the inverse MR. This discontinuity is effected through a normal shock between the reflected wave and the wall (Fig. 3(h) - 3(l)). The normal shock moves downstream relative to the "orphan"shock system. The shock wave system upstream of the normal shock becomes too weak to notice on the density contour plots. The bow wave at the wedge leading edge is now a Prandtl-Meyer expansion whose influence propagates towards the wall resulting in additional wave modification.

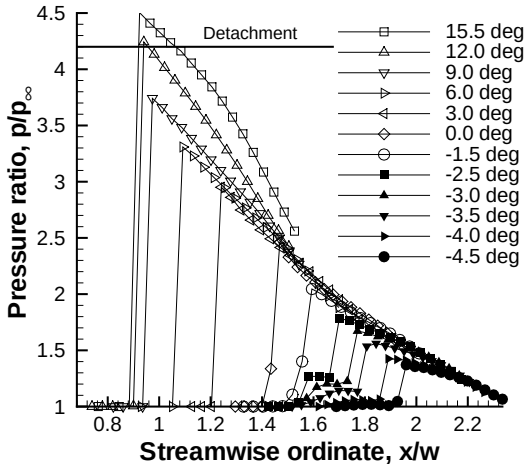

Fig. 5. Unsteady static pressure response on the reflection plane : case 12

3.3 Unsteady static pressure characterization on the reflection plane

Pressure scans through the reflection point on the wall, for case 12, are shown in Fig. 5. As the wedge is pitched about its leading edge, the pressure rise through the reflection point decreases continuously until transition to RR. The pressure rise at transition, θ = -1.5°, is approximately 51.2% below the theoretical detachment condition. Due to the inverse MR configuration observed for these dynamic cases (MR → RR only), a discontinuity in pressure rise is expected across transition. This is achieved through a normal shock that propagates downstream between the reflected shock and the wall. The moving normal shock can be seen in the pressure traces for $\theta <$ -1.5°.

3.4 Unsteady triple point response

MR → RR

M_∞ = 2.0 (Cases 10, 11 and 12): In contrast to case 12, the Mach stem development history for case 11 in Fig. 6(a) demonstrates a noteworthy difference. In case 11 the triple point maintains its initial vertical location. At θ = 13.0° the Mach stem height decreases. Unexpectedly, at approximately θ = 9.0°, the triple point begins to move away from the wall. At approxiamtely θ = 6.5°, the triple point eventually begins its final movement toward the reflection plane. This fundamental difference lies in the fact that the wedge leading edge and incident shock attachment point is fixed for case 12 and moving for case 11. Case 10 demonstrates a similar characteristic to case 11, with the exception that transition to RR occurs at approximately θ = 4.5° due to the smaller pitch rate. Complete understanding of this complex, non-linear phenomena requires detailed understanding of the acoustic properties of the dynamic flow field.
M_∞ = 4.0 (Cases 4, 5 and 6): The triple point response trends in Fig. 6(b) are similar to those observed at M_∞ = 2.0 for rotation about the wedge leading edge and trailing edge.

RR → MR

$M_\infty = 2.0$ (Cases 7, 8 and 9): Mach stem growth in Fig. 6(a) is approximately quadratic. The wedge incidence angle at transition is dependent on pivot point and rotation rate for a specified initial wedge incidence.
$M_\infty = 4.0$ (Cases 1, 2 and 3): Mach stem growth in Fig. 6(b) is approximately linear. Once again, the dependency on rotation rate and pivot point is demonstrated. It is not known, at this stage, whether the Mach stem growth trend is quadratic for larger pitch rates at M_∞=4.0.

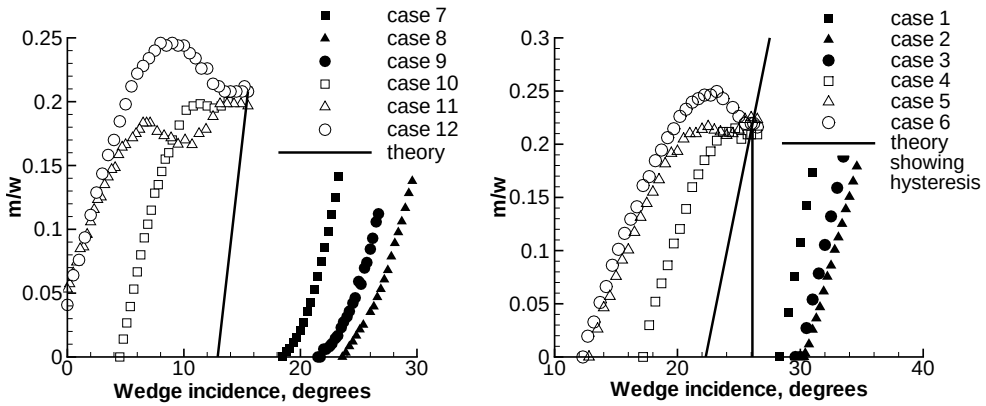

Fig. 6. Dynamic Mach stem growth at (a) $M_\infty = 2.0$ and (b) $M_\infty = 4.0$

4 Conclusion

Transition from MR to RR was demonstrated for the unsteady, "orphan"shock system with CFD. Pressure traces on the reflection plane show, very clearly, the nature of the inverse MR before transition to RR as well as the development and movement of the normal shock between the reflected wave and the reflection plane after transition to RR. Complex triple point behaviour was observed at $M_\infty = 2.0$ and $M_\infty = 4.0$. For a particular freestream condition and initial wedge incidence these phenomena demonstrate a strong dependence on wedge pitch rate, direction of rotation and pivot point.

References

1. Ben-Dor G: Hysteresis phenomena in shock wave reflections in steady flows. **Proceedings, 22nd International Symposium on Shock Waves**, Paper 6000 (1999)
2. Felthun LT, Skews BW: Transition Between Regular and Mach Reflection in Dynamic Compressible Flows. **AIAA Journal**, 2002-0549 (2002)
3. Naidoo K, Skews BW: Dynamic shock reflection phenomena in ideal, two-dimensional flows. **Proceedings, 25th International Symposium on Shock Waves**, Paper 1187 (2005)